Geochemical Modeling of the Mantle Partial Melting using Heuristic Exploration: An Optimization Model Applied to Earth Sciences

Roberto Soto-Villalobos
Universidad Autónoma de Nuevo León
Mario A. Aguirre López
Universidad Autónoma de Chiapas
Otoniel Walle-García
Universidad Autónoma de Nuevo León
Francisco Gerardo Benavides-Bravo
Tecnológico Nacional de México
F-Javier Almaguer-Martínez
Universidad Autónoma de Nuevo León
S. Méndez-Delgado
Universidad Autónoma de Nuevo León
Fernando Velasco-Tapia (fernando.velascotp@uanl.edu.mx)
Universidad Autónoma de Nuevo León

Method Article

Keywords: Mantle, Partial melting, Geochemical modeling, Trace elements, Heuristics, Evolution Strategy

Posted Date: August 4th, 2023

DOI: https://doi.org/10.21203/rs.3.rs-3200966/v1

Additional Declarations: No competing interests reported.

Version of Record: A version of this preprint was published at Earth Science Informatics on November 29th, 2023. See the published version at https://doi.org/10.1007/s12145-023-01171-9.

Geochemical Modeling of the Mantle Partial Melting using Heuristic Exploration: An Optimization Model Applied to Earth Sciences

Roberto Soto-Villalobos[1], Mario A. Aguirre-López[2], Otoniel Walle-García[3], Francisco Gerardo Benavides-Bravo[4], F-Javier Almaguer[3], S. Méndez-Delgado[1], Fernando Velasco-Tapia[1*]

[1]Facultad de Ciencias de la Tierra, Universidad Autónoma de Nuevo León, Carretera a Cerro Prieto km.8, Linares, 67700, Nuevo León, Mexico.

[2]Facultad de Ciencias en Física y Matemáticas, Universidad Autónoma de Chiapas, Carretera Emiliano Zapata km.8, Tuxtla Gutiérrez, 29050, Chiapas, Mexico.

[3]Facultad de Ciencias Físico-Matemáticas, Universidad Autónoma de Nuevo León, Pedro de Alba s/n, San Nicolás de los Garza, 66455, Nuevo León, Mexico.

[4]Instituto Tecnológico de Nuevo León, Tecnológico Nacional de México, Av. Eloy Cavazos 2001, Guadalupe, 67170, Nuevo León, Mexico.

*Corresponding author(s). E-mail(s): fernando.velascotp@uanl.edu.mx; Contributing authors: roberto.sotovll@uanl.edu.mx; marioal1906@gmail.com; owalleg@gmail.com; francisco.bb@nuevoleon.tecnm.mx; francisco.almaguermrt@uanl.edu.mx; sostenes.mendezdl@uanl.edu.mx;

Abstract

An evolution strategy-type heuristic simulation tool was developed to optimize the mantle partial melting inverse modeling. An objective or fitness function was derived from the batch equation to model the source composition and the partial melting degree from the chemistry of near primary liquids. In the search algorithm structure was considered: (a) the geochemical system constraints, (b) an initialization step, and (c) a procedure of mutation and heuristic individual selection. The heuristic simulation was successfully applied in four study cases, as mineralogical and rare earth element (REE) composition of known peridotitic sources. Partial melting conditions were reproduced with a deviation $\leq \mathbf{10^{-6}}$ in a reasonably practical time ($\sim \mathbf{2}$ hours) by using a desktop computer.

Keywords: Mantle, Partial melting, Geochemical modeling, Trace elements, Heuristics, Evolution Strategy

1 Introduction

Mantle partial melting is an essential process to understand the geological evolution of the Earth. Several quantitative geochemical models (i.e., batch and fractional approaches) based on the incompatible element behavior have been proposed about half a century ago [1–3]. Batch melting assumes that melt remains in equilibrium with the residual solid through the event. In contrast, fractional melting assumes that the melt is constantly removed from the source as it is formed. Recently, [4] implemented PetroGram, an Excel program to carry out inverse partial melting modeling. More complex models have been suggested such as the continuous or critical melting model [5–9], where an excess melt is removed from the static mantle source, or the dynamic melting [10–12], in which the entire melting region migrates and new fertile material is incorporated into the source. [13] reported a comprehensive review of all these mantle partial melting models. [14] carried out an inverse scheme with a Markov chain Monte Carlo sampling method to simulate temperature and mantle composition during an adiabatic decompression melting of pyroxenite-bearing peridotite sources. A Markov chain Monte Carlo algorithm was also applied in a partial melting probabilistic inversion strategy by [15]. This approach was used to establish major and rare earth element composition of source and melting conditions.

However, these forward models (batch, fractional, or continuous/dynamic melting) attempt to duplicate (essentially by trial and error in the basic cases) the observed trace element composition in near primary magmas derived from the parental source, without later modification by differentiation processes [16]. As a result, the application of these models involves several parameters: the mineralogical and chemical composition of the peridotite, the degree of melting, partition coefficients, or the relative participation of the mineralogical phases during the process.

As a methodological answer to forward model restrictions, several inverse approaches also have been developed. Their main objective is to reduce the number of parameters observed in the forward approaches to reach a consistent view. Based on a limited number of geochemical assumptions, the mineralogical and geochemical composition of the parental source, as well as partial melting conditions, are established from the variations in incompatible trace element concentrations of a cogenetic suite of rocks produced by different degrees of melting [13]. [17] and [18] reported an inverse approach, based on enrichment concentration ratios of incompatible elements, to establish the degrees of partial melting. Nevertheless, the source ratio or linear regression approach has been the inverse method most commonly used [19, 20]. [21–32] are some case studies that used such a method, although they only dealt with batch melting (i.e., fractional or dynamic melting cannot be expressed by linear equations). However, the linear equations of the source ratio approach may be affected by the uncertainty associated with intercept and slope algebraic estimation [33, 34]. Additionally, these complex linear systems do not have a unique solution. As a consequence, a basic problem is to prove that geochemically consistent and valid results can be obtained from the partial melting modeling.

On the other hand, in mathematical modeling, an optimization problem makes use of an objective function and a set of variables to re-define the way of solving a problem, so that, the problem consists of finding the combination of variables (a solution) that minimizes that function, within the entire set of possible solutions. Then, there are multiple different strategies or methodologies to solve this type of problem among which heuristic techniques arise, see [35] and references therein.

According to [36], a heuristic is an iterative solution approach by trial and error that produces acceptable solutions to a complex problem in a reasonably practical time. In this sense, heuristic techniques deal with the complexity of the problem by improving the optimal solution found in each iteration instead of carrying out an exhaustive search throughout the feasible solution space. Taking into account that there is no guarantee that the best solution(s) can be found, the idea is then to apply a heuristic technique that brings an optimal solution for the specific problem at the end of the iterative process.

Now, even though there are a lot of heuristic techniques and their use is very common in some areas of science, it is important to note that the application of heuristics in earth sciences is still limited. Only a few case studies have been reported in different sub-areas, such as Pattern Search (PS) applied to aero-geophysical data analysis [37]; Particle Swarm Optimization (PSO), Genetic Algorithms (GAs), Harmony Search (HS), Generalized Simulated Annealing (GSA), and PS applied to hydrology/hydrogeology [38–40]; GA applied to meteorology [41]; Spiral Optimization (SO), Gravitational Search (GSA), Bath Algorithm (BA), GA, PSO, and Artificial Neuronal Networks (ANN) and Support Vector Machine (SVM) algorithms applied to seismic/seismology [42–45]. To our knowledge, there is only one work reported about the use of heuristics in geochemistry [46], in which Ant Colony Optimization (ACO) was used to properly identify geochemical anomalies.

In the present study, an evolution strategy-type heuristic simulation and validation were established to optimize the mantle partial batch melting inversion modeling using the rare earth element (REE) geochemistry. This element group shows a marked incompatible behavior concerning the usual mineralogy observed in the Earth's mantle [8]. The heuristic approach was successfully applied to obtain the mineralogical and geochemical composition of the parental source and the degree of partial melting event related to each daughter rock. The structure of the paper is as follows: Section 2 explains the modeling and construction of the optimization problem; Section 3 details the heuristic and parameters used to solve the problem; finally, Section 4 discusses the resulting simulations, while Section 5 shows the concluding remarks.

2 Batch Partial Melting Equation as an Optimization Problem

Considering the incompatible trace elements *La, Ce, Pr, Nd, Sm, Eu, Gd, Tb, Dy, Ho, Er, Tm, Yb, Lu*, [3] proposed the following distribution equation to evaluate the concentration C_L^i of the i-th trace element in a melt, which is produced by the Mantle partial modal melting in a closed system condition, as:

$$C_L^i = \frac{C_0^i}{F + (1-F)D_0^i} \qquad \forall i \in \{La, Ce, \ldots, Lu\}, \tag{1}$$

where D_0^i is the bulk partition coefficient, C_0^i represents the concentration of the i-th incompatible trace element in the chemical composition of the Mantle source, and F is the partial melting percentage.
Shaw´s equation (1) is restricted to magmatic systems following the next working assumptions:

(a) the magma and the residual solid are in chemical equilibrium through the whole partial melting process until the liquid is segregated (and then, exists a concentration C_0^i of the solid source if the i-th element is considered),
(b) before the melting process starts, a mass proportion of the initial solid is converted into a magmatic liquid (the existence of a degree of partial melting F),
(c) each incompatible trace element satisfy a mass balance equation, i.e., the fulfillment of the Equation (1).

In this manner, the next restrictions must be satisfied:

$$C_0^i > 0 \qquad \forall i \in \{La, Ce, \ldots, Lu\}, \tag{2}$$
$$F \in (0, 1], \tag{3}$$

taking both, C_0^i and F, a positive value because of restrictions (a) and (b), respectively. Now, since the peridotitic source is constituted by n minerals (at least: olivine, orthopyroxene, clinopyroxene, and an Al-bearing mineral phase), each of them must consist of a proportion of the entire rock, such that:

$$x^j > 0.0 \qquad \forall j \in \{1, \ldots, n\} \tag{4}$$

and

$$\sum_{j=1}^{n} x^j = 1.0. \tag{5}$$

In this way, each i-th trace element is characterized by a bulk partition coefficient D_0^i, which is associated with the weighted sum of mineral proportions x_j's by

$$D_0^i = \sum_{j=1}^{n} x^j K_j^i \qquad \forall i \in \{La, Ce, \ldots, Lu\}, \tag{6}$$

where K_j^i is weight partition coefficient of the $j-$th mineral for the $i-$th trace element. Finally, Shaw´s equation (1) could be rewritten as the expression:

$$\frac{C_0^i}{F+(1-F)D_0^i} - C_L^i = 0 \qquad \forall i \in \{La, Ce, \ldots, Lu\}, \tag{7}$$

which should be equal to zero or any absolute value close to it, i.e., $\sim 10^{-12}$ to 10^{-9}, for an ideal condition. Taking this into account and integrating several i-elements in Equation (7), it results:

$$\sum_{i=La}^{Lu} \left| \frac{C_0^i}{F+(1-F)D_0^i} - C_L^i \right| \approx 0.0. \tag{8}$$

Thus, the objective function for a specific magmatic liquid, based on the REE geochemistry, is established as:

$$f_{obj}(F, x^1, x^2, \ldots, x^n, C_0^{La}, C_0^{Ce}, \ldots, C_0^{Lu}) = \sum_{i=La}^{Lu} \left| \frac{C_0^i}{F+(1-F)D_0^i} - C_L^i \right| \tag{9}$$

which depends on $\dim\{La, Ce, \ldots, Lu\} + n + 1$ variables, and it is subjected to the constraints of:

- Equation (2): existence of the solid source for each i-th trace element with a certain concentration C_0^i,
- Equation (3): existence of the partial melting phenomenon in a certain degree F,
- Equation (4): existence of each j-th mineral considered in a certain proportion x^j,
- Equation (5): the unity of the rock that is composed of a total of j minerals.

3 Heuristic technique: Evolution Strategy

Evolution Strategy (*ES*) was used to solve the optimization problem described by the objective function (9), starting from a primary liquid magma population. *ES* is a heuristic that belongs to the larger class of evolutionary algorithms, and like other heuristics in this group, they imitate adaptive biological evolution processes. The implementation of variation and selection operators in *ES* searches is distinctive. The variation operator that produces new individuals is, in this case, the mutation operator. The selection operator chooses the best individuals from a population based on the fitness value that corresponds to each individual, which is calculated using the objective function. The next population is created from the chosen individuals, and the procedure is repeated; see [47] and references therein for further information. The steps of the *ES* algorithm are illustrated in Figure 1. It consists of a typical heuristic algorithm with initialization, mutation, selection, and stop criteria steps. In addition, we established the conditions for obtaining feasible solutions (constraints of the partial melting problem) in each generation. Next, we will describe each step of the *ES* algorithm in depth.

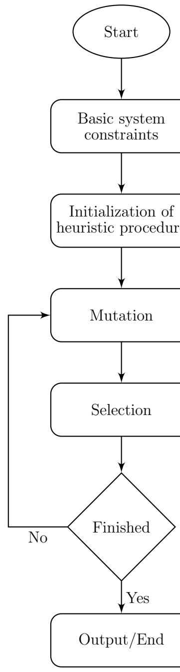

Fig. 1 Flowchart of the *ES* implementation.

3.1 Initial population

This stage begins with a set of solutions (or heuristic individuals) generated at random that fulfill the restrictions imposed on the system. Thus, a heuristic individual is defined as a real number vector constituted by several components:

1. the partial melting percentage,
2. the modal composition of the Mantle source,
3. the REE chemical composition of the Mantle source.

Therefore, a fitness-of-solution is computed for each heuristic individual. Initially, the user should set the REE partition coefficients. The method starts the search process for REE composition in the Mantle source by selecting a random solution from a decision space.

3.2 Mutation

This is the most important heuristic step, as the individual success of the search depends on it. Throughout the mutation process, for example, two mineral phase proportions are randomly selected. A quantity is added to the first variable, whereas a similar value is reduced to the second mineral phase proportion. Clearly, the solution for each of the n modal proportions is constrained to the $(0,1]$ range, yielding the Cartesian product $(0,1] \times (0,1] \times \cdots \times (0,1] = (0,1]^n$ as the global search space. The real numbers in the $(0,1]$ range are reported as $0.d_1d_2d_3 \ldots d_{14}$ (i.e., each numeric solution has been represented by fourteen digits after the decimal point). For each digit d_n, a group of 1000 random numbers (i.e., the search space for the digit) has been generated between the quantities a and b characterized by a uniform distribution. Therefore, the "discrete jump" mutation is defined by the addition or subtraction of these random numbers to the original digit d_n. This process has been extended to the fourteen decimals ($\pm 10^{-n}$) by the function $msd(1, 14)$, repeatedly up to a maximum of 5×10^4 iterations.

3.3 Selection

The fitness-of-solution for each heuristic individual is determined by the proximity to a zero value in the evaluation of Equation (9). Being an elitist procedure, in each stage the algorithm computes the objective function at the mesh points and selects one whose value is better than the first solution's objective function value. If there is a solution with a better objective function in the newly generated solutions, the searching point will be transferred to the mesh points, while the worst obtained solution is discarded.

3.4 Stop criteria

As anticipated, the stop criteria were established by the number of iterations, so that the algorithm ends its operation when reaching 5×10^4 iterations. The heuristic algorithm performance (HAP), i.e., the closeness of the modeled values (mean $\acute{x}$ accompanied with 99% upper and lower confidence levels; LCL and UCL have been calculated following the basic statements of the Central Limit Theorem; [48] predicted by the heuristic approach to the observed ones (μ), can be easily measured in terms the percentage of its normalized difference:

$$HAP = \frac{\acute{x}_F - \mu}{\mu} \times 100, \tag{10}$$

where F is the degree of partial melting.

4 Study Cases and Discussion

For this study, we considered two types of rocks: peridotite, which has partial melting percentages not higher than 20% [8], and ultrabasic liquid rocks with percentages not higher than 60% [49]; felsic and iron-rich components preferentially enter the melt, while the liquid formed has a basaltic composition. We used this knowledge to make the most of the construction of the optimization problem so that the considered range of values in Restriction (3) is modified to:

$$F \in (0, 0.2] \qquad \text{for peridotite, and} \tag{11}$$

$$F \in (0, 0.6] \qquad \text{for ultrabasic liquid rocks.} \tag{12}$$

Specifically, four rocks with mineral and chemical compositions available in the literature were selected as our study cases [50, 51]. They are detailed in Table 1. To initialize the search of solutions, REE composition of primary liquids was generated from each rock using the batch partial melting Equation (1) (forward modeling), taking into account three levels of degree of melting $F = 0.05, 0.10, 0.15$, and the partition coefficients reported by [52] and [53], see Table 2.

In this way, inverse modeling was performed by applying the heuristic simulator described in Section 3 to solve the optimization model described in Section 2, and customized for the study cases, namely, Objective function (9) and Restrictions (2),(4), (5), (11), (12).

Results are summarized in Tables 3-6. Mean ($\acute{x}$) and 99% ($\alpha = 0.01$) lower and upper confidence levels (LCL and UCL values) were established for modeled parameters (sample size = 1000), being contrasted with the original Mantle source and process features. Obtained simulation data for the peridotite JP-1 are representative of the general analysis and are therefore discussed in depth.

The mean values of degree of melting, mineralogical, and REE composition modeled with our technique did not show significant differences compared to the source data [50], as seen in Figures 2 and 3. Moreover, Figure 4 shows that the associated fitness to heuristic search minimizes the objective function after 5×10^4 iterations in ~ 2 hours. The search is robust in the sense that the best, worst, and mean aptitudes evolved satisfactorily from $\sim 10^{-2}$ at ≤ 2000 iterations to $\sim 10^{-13}$ at the end, i.e., there is a low variance with a general convergence. In a similar way for the rest of the cases, the minimal value of the fitness-of-solution was between $\sim 10^{-10}$ to 10^{-12}. That precision reached around 30,000 iterations. Due to the nearer-to-zero values, higher precision is associated with numerical errors.

Chondrite-normalized REE patterns of Figure 5 also confirmed the efficiency of the heuristic simulator as the modeled compositions closely reproduce the distinctive shape, strongly depleted in middle REE (Sm to Dy), for the normalized pattern for JP-1. For all studied cases, the heuristic procedure overvalued slightly the original REE concentrations. The direct comparison of the modeled source composition and the original JP-1 data, using the HAP parameter = $[(JP1F - JP1)/JP1] \times 100$ where $F = 0.05$, 0.10 or 0.15 degree of melting, revealed acceptable differences in composition $< 4\%$ in all REE. However, the comparison for the degree of melting and modal composition yielded deviations of $< 6\%$ and $< 3\%$ respectively. Similar results have been observed in the analysis of the lherzolites 110.1 Lhz, 110.2 Lhz, and 110.3 Lhz, Tables 4, 5 and 6, respectively.

Table 1 Mineralogical and REE geochemical composition for our study cases.

Peridotite	JP-1[1]	110.1Lhz[2]	110.2Lhz[2]	110.3Lhz[2]
Mineralogy (modal %)				
Olivine (Ol)	60	61	75	71
Orthopyroxene (Opx)	10	18	16	15
Clinopyroxene (Cpx)	30	13	7	8
Plagioclase (Plg)		7	1	5
Spinel (Sp)		1	1	1
Rare Earth Elements (ppm)				
La	0.027	0.159	0.015	0.134
Ce	0.060	0.730	0.089	0.614
Pr	0.008	0.184	0.033	0.110
Nd	0.031	1.232	0.244	0.583
Sm	0.009	0.623	0.126	0.217
Eu	0.002	0.249	0.050	0.094
Gd	0.010	0.905	0.207	0.326
Tb	0.002	0.181	0.042	0.066
Dy	0.015	1.307	0.297	0.456
Ho	0.004	0.304	0.068	0.102
Er	0.013	0.874	0.205	0.301
Tm	0.003	0.134	0.035	0.049
Yb	0.022	0.868	0.230	0.318
Lu	0.004	0.136	0.037	0.050

[1]Modal composition assumed in the present work; REE geochemical data from [50].

[2]Modal and REE geochemical data from [51].

Table 2 REE partition coefficients.

Mineral[1]	Olivine	Orthopyroxene	Clinopyroxene	Plagioclase	Spinel
La	0.0035	0.0070	0.1200	0.1000	0.0100
Ce	0.0036	0.0040	0.1700	0.0720	0.0100
Pr	0.0003	0.0095	0.0700	0.1000	0.0100
Nd	0.0050	0.0114	0.3100	0.0500	0.0100
Sm	0.0006	0.0230	0.4900	0.0360	0.0100
Eu	0.0100	0.0250	0.4800	0.2600	0.0100
Gd	0.0041	0.0250	0.4900	0.0300	0.0100
Tb	0.0080	0.0550	0.6400	0.0280	0.0100
Dy	0.0130	0.0800	0.7000	0.0220	0.0100
Ho	0.0100	0.1600	0.6600	0.0110	0.0100
Er	0.0220	0.1500	0.6800	0.0400	0.0100
Tm	0.0400	0.3400	0.8000	0.0100	0.0100
Yb	0.0260	0.0800	0.6200	0.0130	0.0100
Lu	0.0410	0.2000	0.6000	0.0150	0.0100

[1]Data from [53]. A value of 0.01 has been considered for spinel-melt REE partition coefficients from [52].

Table 3 Original mineralogical and REE chemical composition of peridotite $JP-1$ (μ) and those modeled ($\acute{x}$ and 99% confidence levels: LCL = lower, UCL = upper) by the heuristic approach from melts generated at degrees of melting $F = 0.05, 0.10, 0.15$.

		$F = 0.05$			$F = 0.10$			$F = 0.15$		
	μ	$\acute{x}_{0.05}$	LCL	UCL	$\acute{x}_{0.1}$	LCL	UCL	$\acute{x}_{0.15}$	LCL	UCL
F		0.053	0.051	0.055	0.103	0.101	0.105	0.152	0.15	0.154
x^{ol}	0.6	0.599	0.596	0.602	0.597	0.593	0.601	0.599	0.595	0.603
x^{opx}	0.1	0.1	0.097	0.103	0.099	0.096	0.102	0.097	0.094	0.1
x^{cpx}	0.3	0.3	0.297	0.303	0.303	0.3	0.306	0.304	0.3	0.308
C_0^{La}	0.027	0.028	0.0276	0.0284	0.0276	0.0273	0.0279	0.0274	0.0272	0.0276
C_0^{Ce}	0.06	0.062	0.061	0.063	0.0613	0.0606	0.062	0.0609	0.0604	0.0614
C_0^{Pr}	0.0077	0.008	0.0078	0.0082	0.0078	0.0077	0.0079	0.0078	0.0077	0.0079
C_0^{Nd}	0.031	0.0317	0.0314	0.032	0.0316	0.0314	0.0318	0.0314	0.0313	0.0315
C_0^{Sm}	0.0088	0.00894	0.00888	0.009	0.00895	0.00889	0.00901	0.00892	0.00888	0.00896
C_0^{Eu}	0.0024	0.00244	0.00242	0.00246	0.00244	0.00242	0.00246	0.00243	0.00242	0.00244
C_0^{Gd}	0.01	0.01016	0.0101	0.01022	0.01017	0.01011	0.01023	0.01013	0.01009	0.01017
C_0^{Tb}	0.002	0.00202	0.00201	0.00203	0.00203	0.00202	0.00204	0.00202	0.00201	0.00203
C_0^{Dy}	0.015	0.0152	0.0151	0.0153	0.0152	0.0151	0.0153	0.0152	0.0151	0.0153
C_0^{Ho}	0.0037	0.00374	0.00373	0.00375	0.00376	0.00374	0.00378	0.00374	0.00373	0.00375
C_0^{Er}	0.013	0.0131	0.013	0.0132	0.0132	0.0131	0.0133	0.0131	0.013	0.0132
C_0^{Tm}	0.0026	0.00262	0.00261	0.00263	0.00263	0.00262	0.00264	0.00262	0.00261	0.00263
C_0^{Yb}	0.022	0.0223	0.0222	0.0224	0.0223	0.0222	0.0224	0.0222	0.022	0.0224
C_0^{Lu}	0.0043	0.00435	0.00433	0.00437	0.00436	0.00434	0.00438	0.00435	0.00433	0.00437

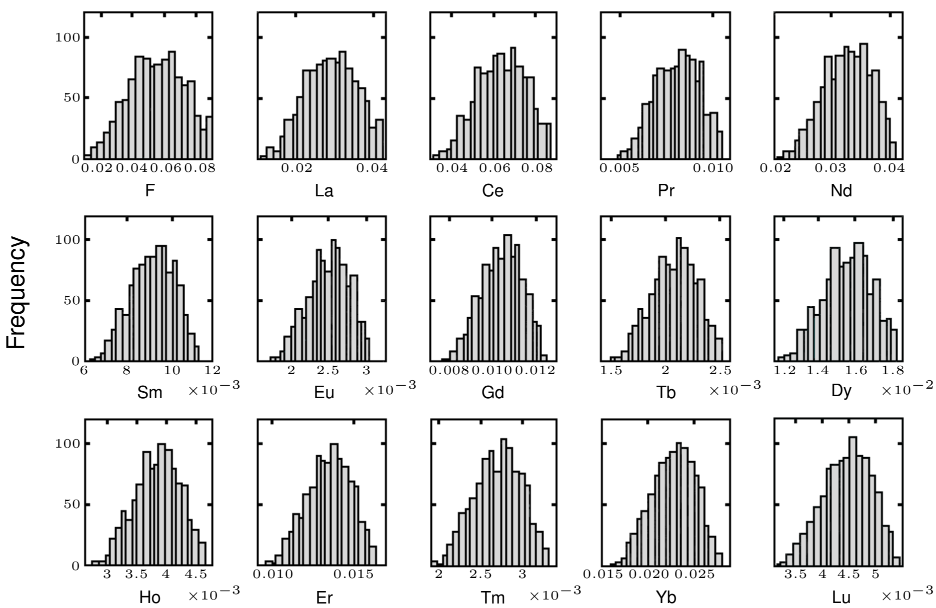

Fig. 2 Histogram data distribution modeled for peridotite JP-1 at $F = 0.10$.

Table 4 Original mineralogical and REE chemical composition of peridotite TFI 110.1 (μ) and those modeled ($\acute{x}$ and 99% confidence levels: LCL = lower, UCL = upper) by the heuristic approach from melts generated at degrees of melting $F = 0.05, 0.10, 0.15$.

		$F = 0.05$			$F = 0.10$			$F = 0.15$		
	μ	$\acute{x}_{0.05}$	LCL	UCL	$\acute{x}_{0.1}$	LCL	UCL	$\acute{x}_{0.15}$	LCL	UCL
F		0.051	0.049	0.053	0.099	0.098	0.1	0.149	0.148	0.152
x^{ol}	0.61	0.607	0.605	0.609	0.606	0.603	0.609	0.608	0.605	0.611
x^{opx}	0.18	0.178	0.176	0.18	0.177	0.175	0.179	0.178	0.176	0.18
x^{cpx}	0.13	0.132	0.13	0.134	0.134	0.132	0.136	0.132	0.13	0.134
x^{plg}	0.07	0.073	0.071	0.075	0.073	0.071	0.075	0.072	0.07	0.074
x^{sp}	0.01	0.0099	0.0096	0.0102	0.01	0.0098	0.0102	0.0099	0.0097	0.0101
C_0^{La}	0.159	0.162	0.159	0.165	0.16	0.158	0.162	0.159	0.157	0.161
C_0^{Ce}	0.73	0.744	0.731	0.756	0.734	0.724	0.744	0.73	0.722	0.738
C_0^{Pr}	0.184	0.188	0.184	0.192	0.185	0.182	0.188	0.184	0.182	0.186
C_0^{Nd}	1.23	1.254	1.24	1.269	1.243	1.229	1.257	1.234	1.224	1.244
C_0^{Sm}	0.623	0.634	0.628	0.64	0.63	0.625	0.635	0.625	0.621	0.629
C_0^{Eu}	0.249	0.254	0.252	0.256	0.252	0.25	0.254	0.25	0.249	0.251
C_0^{Gd}	0.905	0.921	0.913	0.929	0.915	0.908	0.922	0.908	0.901	0.915
C_0^{Tb}	0.181	0.184	0.183	0.185	0.183	0.182	0.184	0.182	0.181	0.183
C_0^{Dy}	1.307	1.327	1.319	1.335	1.323	1.315	1.331	1.312	1.305	1.319
C_0^{Ho}	0.304	0.308	0.306	0.31	0.307	0.305	0.309	0.305	0.303	0.307
C_0^{Er}	0.874	0.885	0.88	0.89	0.883	0.878	0.888	0.877	0.872	0.882
C_0^{Tm}	0.134	0.135	0.134	0.136	0.135	0.134	0.136	0.134	0.133	0.135
C_0^{Yb}	0.868	0.88	0.874	0.886	0.877	0.871	0.883	0.871	0.866	0.876
C_0^{Lu}	0.136	0.137	0.136	0.138	0.137	0.136	0.138	0.136	0.135	0.137

5 Conclusions

Detailed knowledge about the Mantle partial melting and magma generation is an important issue in igneous petrology. In this paper, a heuristic optimization technique was used to solve the Mantle batch partial melting inverse problem. The proposed Evolution Strategy algorithm has the potential to provide, in a reasonably practical time ($\sim$ 2 hours), efficient solutions for the mineralogical and geochemical composition of peridotitic source and the partial melting degree.

Modeled REE composition of the peridotitic source showed small deviations $\leq$ 4% concerning expected values reported in the literature. A comparable efficiency was observed for the modal source composition ($<$ 6%) and degree of melting modeling ($<$ 3%).

The heuristic methodology is flexible in construction, having the property of being easily adapted to solve complex optimization Mantle partial melting problems (i.e., fractional or dynamic models) successfully and efficiently. This joined to our acceptable results, suggests the use of similar heuristic algorithms as tools in the evaluation of evolution magmatic processes, such as fractional crystallization, assimilation, or magma mixing/mingling.

Funding. This work was partially supported by a grant from the PAICyT-UANL program (Project no. CT786-02); and by Facultad de Ciencias de la Tierra, Universidad Autónoma de Nuevo León (FCT-UANL), without a special grant number.

Table 5 Original mineralogical and REE chemical composition of peridotite TFI 110.2 (μ) and those modeled ($\acute{x}$ and 99% confidence levels: LCL = lower, UCL = upper) by the heuristic approach from melts generated at degrees of melting $F = 0.05, 0.10, 0.15$.

		$F = 0.05$			$F = 0.10$			$F = 0.15$		
	μ	$\acute{x}_{0.05}$	LCL	UCL	$\acute{x}_{0.1}$	LCL	UCL	$\acute{x}_{0.15}$	LCL	UCL
F		0.05	0.048	0.052	0.099	0.097	0.101	0.149	0.147	0.151
x^{xol}	0.75	0.758	0.756	0.76	0.758	0.756	0.76	0.759	0.757	0.761
x^{opx}	0.16	0.136	0.134	0.138	0.136	0.135	0.137	0.137	0.136	0.138
x^{cpx}	0.07	0.086	0.083	0.089	0.084	0.082	0.086	0.083	0.081	0.085
x^{plg}	0.01	0.0106	0.0103	0.0109	0.0103	0.0101	0.0105	0.0103	0.0101	0.0105
x^{sp}	0.01	0.0103	0.01	0.0106	0.0102	0.01	0.0104	0.0103	0.01	0.0106
C_0^{La}	0.015	0.0154	0.0149	0.0159	0.0151	0.0148	0.0154	0.0151	0.0149	0.0153
C_0^{Ce}	0.089	0.092	0.089	0.095	0.09	0.089	0.091	0.09	0.089	0.091
C_0^{Pr}	0.033	0.033	0.032	0.034	0.033	0.032	0.034	0.033	0.032	0.034
C_0^{Nd}	0.244	0.258	0.252	0.264	0.251	0.248	0.254	0.248	0.246	0.25
C_0^{Sm}	0.126	0.135	0.133	0.137	0.131	0.13	0.132	0.129	0.128	0.13
C_0^{Eu}	0.05	0.053	0.052	0.054	0.052	0.051	0.053	0.051	0.05	0.052
C_0^{Gd}	0.207	0.222	0.216	0.228	0.215	0.213	0.217	0.212	0.211	0.213
C_0^{Tb}	0.042	0.045	0.044	0.046	0.044	0.043	0.045	0.043	0.042	0.044
C_0^{Dy}	0.297	0.318	0.314	0.322	0.31	0.307	0.313	0.306	0.304	1.308
C_0^{Ho}	0.068	0.071	0.07	0.072	0.07	0.069	0.071	0.069	0.068	0.07
C_0^{Er}	0.205	0.215	0.213	0.217	0.212	0.211	0.213	0.209	0.208	0.21
C_0^{Tm}	0.035	0.036	0.035	0.037	0.036	0.035	0.037	0.0354	0.0352	0.0356
C_0^{Yb}	0.23	0.244	0.241	0.247	0.239	0.237	0.241	0.236	0.234	0.238
C_0^{Lu}	0.037	0.038	0.037	0.039	0.038	0.037	0.039	0.0374	0.0372	0.0376

Conflict of Interest Statement. The authors declare that the research was conducted in the absence of any commercial or financial relationships that could be construed as a potential conflict of interest.

Availability of data and material. The datasets generated for this study will be provided upon request to the corresponding author.

Authors' Contributions. RS-V: Conceptualization, Investigation, Methodology, Resources, Funding, Writing – original draft, Software, Formal analysis, Data Visualization. MAA-L: Writing – review & editing, Formal analysis, Validation. OW-G: Data Visualization, Writing – review & editing, Validation. FGB-B: Writing – review & editing, Validation. F-JA: Writing – review & editing, Validation. SM-D: Resources, Funding, Writing – review & editing, Supervision. FV-T: Conceptualization, Investigation, Project administration, Resources, Funding, Writing – original draft, Formal analysis.

Acknowledgments. RS-V. and O.W.-G. thank CONACyT for their scholarships, while MAA-L. thanks CONACyT for his postdoctoral grant 839412. All the authors express their gratitude to Pablo Antonio Ramírez-Trejos for his English editing support.

Table 6 Original mineralogical and REE chemical composition of peridotite TFI 110.3 (μ) and those modeled ($\acute{x}$ and 99% confidence levels: LCL = lower, UCL = upper) by the heuristic approach from melts generated at degrees of melting $F = 0.05, 0.10, 0.15$.

		F = 0.05			F = 0.10			F = 0.15		
	μ	$\acute{x}_{0.05}$	LCL	UCL	$\acute{x}_{0.1}$	LCL	UCL	$\acute{x}_{0.15}$	LCL	UCL
F		0.051	0.049	0.053	0.1	0.098	0.102	0.151	0.149	0.153
x^{ol}	0.71	0.704	0.702	0.706	0.707	0.705	0.709	0.707	0.705	0.709
x^{opx}	0.15	0.148	0.145	0.151	0.148	0.146	0.15	0.15	0.147	0.153
x^{cpx}	0.08	0.087	0.085	0.089	0.083	0.081	0.085	0.082	0.08	0.084
x^{plg}	0.05	0.052	0.05	0.054	0.052	0.05	0.054	0.051	0.049	0.053
x^{sp}	0.01	0.0098	0.0096	0.01	0.0097	0.0095	0.0099	0.0098	0.0095	0.0101
C_0^{La}	0.134	0.137	0.134	0.14	0.135	0.133	0.137	0.135	0.133	0.137
C_0^{Ce}	0.614	0.631	0.617	0.645	0.619	0.609	0.629	0.618	0.612	0.624
C_0^{Pr}	0.11	0.112	0.109	0.115	0.111	0.109	0.113	0.111	0.109	0.113
C_0^{Nd}	0.583	0.604	0.593	0.613	0.589	0.581	0.597	0.588	0.582	0.594
C_0^{Sm}	0.217	0.226	0.223	0.229	0.22	0.217	0.223	0.219	0.217	0.221
C_0^{Eu}	0.094	0.098	0.097	0.099	0.095	0.094	0.096	0.095	0.094	0.096
C_0^{Gd}	0.326	0.34	0.335	0.345	0.33	0.327	0.333	0.329	0.326	0.332
C_0^{Tb}	0.066	0.069	0.068	0.07	0.067	0.066	0.068	0.0667	0.0662	0.0672
C_0^{Dy}	0.456	0.475	0.471	0.479	0.462	0.458	0.466	0.461	0.458	0.464
C_0^{Ho}	0.102	0.106	0.105	0.107	0.103	0.102	0.104	0.103	0.102	0.104
C_0^{Er}	0.301	0.312	0.310	0.314	0.305	0.302	0.308	0.304	0.302	0.306
C_0^{Tm}	0.049	0.0503	0.050	0.0506	0.0495	0.0491	0.0499	0.0494	0.0492	0.0496
C_0^{Yb}	0.318	0.330	0.326	0.334	0.322	0.319	0.325	0.321	0.319	0.323
C_0^{Lu}	0.030	0.0308	0.0305	0.0311	0.0302	0.03	0.0304	0.0302	0.03	0.0304

References

[1] Schilling, J.-G., Winchester, J.W.: Rare-earth fractionation and magmatic processes. In: Runcorn, S.K. (ed.) Mantles of the Earth and Terrestrial Planets, vol. 67-26566, pp. 267–283 (1967)

[2] Gast, P.W.: Trace element fractionation and the origin of tholeiitic and alkaline magma types. Geochimica et Cosmochimica Acta **32**(10), 1057–1086 (1968) https://doi.org/10.1016/0016-7037(68)90108-7

[3] Shaw, D.M.: Trace element fractionation during anatexis. Geochimica et Cosmochimica Acta **34**(2), 237–243 (1970) https://doi.org/10.1016/0016-7037(70)90009-8

[4] Gündüz, M., Asan, K.: Petrogram: An excel-based petrology program for modeling of magmatic processes. Geoscience Frontiers **12**(20210106), 81 (2021) https://doi.org/10.1016/j.gsf.2020.06.010

[5] Maaløe, S.: Geochemical aspects of permeability controlled partial melting and fractional crystallization. Geochimica et Cosmochimica Acta **46**(1), 43–57 (1982) https://doi.org/10.1016/0016-7037(82)90289-7

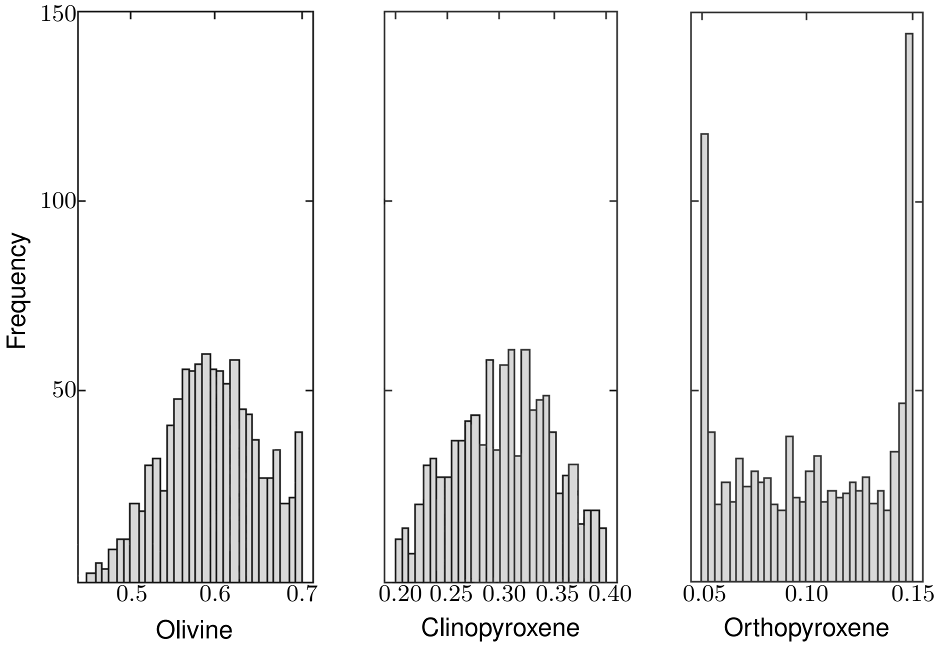

Fig. 3 Histogram of modal composition for the peridotitic source, JP-1 at $F = 0.10$.

[6] W. Williams, R., B. Gill, J.: Effects of partial melting on the uranium decay series. Geochimica et Cosmochimica Acta **53**(7), 1607–1619 (1989) https://doi.org/10.1016/0016-7037(89)90242-1

[7] Sobolev, A.V., Shimizu, N.: Ultra-depleted primary melt included in an olivine from the mid-atlantic ridge. Nature **363**(6425), 151–154 (1993) https://doi.org/10.1038/363151a0

[8] Albarède, F.: Introduction to Geochemical Modeling. Cambridge University Press, Cambridge (1995). https://doi.org/10.1017/CBO9780511622960

[9] Shaw, D.M.: Continuous (dynamic) melting theory revisited. The Canadian Mineralogist **38**(5), 1041–1063 (2000) https://doi.org/10.2113/gscanmin.38.5.1041 https://pubs.geoscienceworld.org/canmin/article-pdf/38/5/1041/3420807/1041_vol38-5_art_01.pdf

[10] Langmuir, C.H., Bender, J.F., Bence, A.E., Hanson, G.N., Taylor, S.R.: Petrogenesis of basalts from the FAMOUS area: Mid-Atlantic Ridge. Earth and Planetary Science Letters **36**(1), 133–156 (1977) https://doi.org/10.1016/0012-821X(77)90194-7

[11] Zou, H.: Trace element fractionation during modal and nonmodal dynamic melting and open-system melting: a mathematical treatment. Geochimica

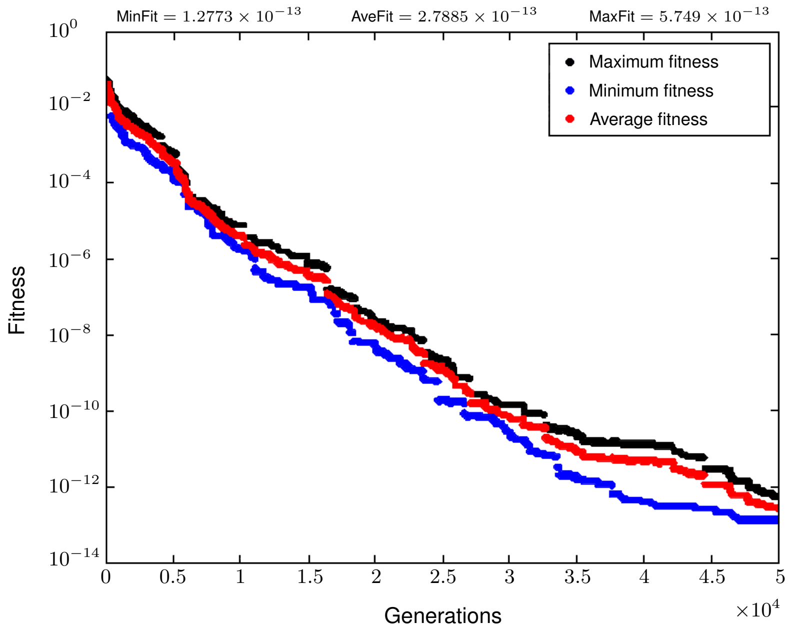

Fig. 4 Solution distribution of the maximum, minimum, and average fitness in the peridotite $JP-1$ with $K = K1$ and $F = 0.05$. MinFit, AveFit, and MaxFit are the minimum, average, and maximum fitness values of the last generation, respectively.

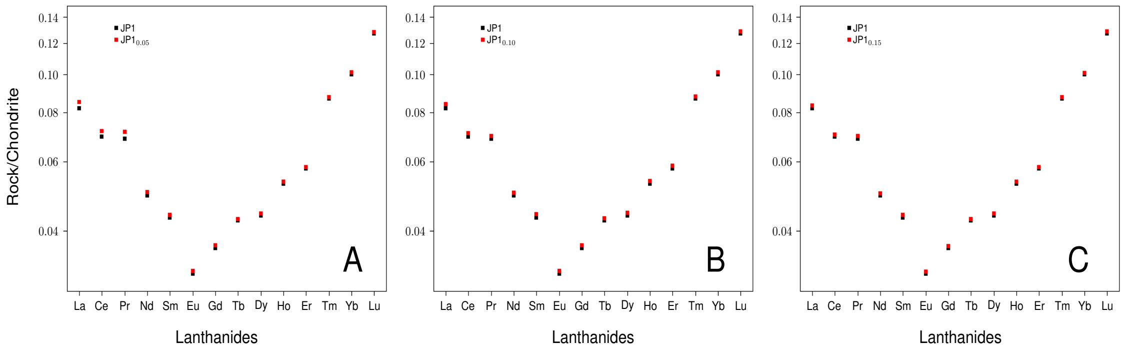

Fig. 5 Chondrite-normalized REE plots for peridotite JP-1; original composition (black square) reported by [50] and average modeled by the heuristic approach (red square): (A) $F = 0.05$, (B) $F = 0.10$, and (C) $F = 0.15$. Average chondrite values (ppm) used for normalization are from [54] and [55]: $La = 0.329$, $Ce = 0.865$, $Pr = 0.112$, $Nd = 0.630$, $Sm = 0.203$, $Eu = 0.077$, $Gd = 0.276$, $Tb = 0.047$, $Dy = 0.343$, $Ho = 0.070$, $Er = 0.225$, $Tm = 0.030$, $Yb = 0.220$, and $Lu = 0.0339$.

et Cosmochimica Acta **62**(11), 1937–1945 (1998) https://doi.org/10.1016/S0016-7037(98)00115-X

[12] Zou, H.: Modeling of trace element fractionation during non-modal dynamic melting with linear variations in mineral/melt distribution coefficients. Geochimica et Cosmochimica Acta **64**(6), 1095–1102 (2000) https://doi.org/10.1016/S0016-7037(99)00383-X

[13] Zou, H.: Quantitative Geochemistry. Published by Imperial College Press and distributed by World Scientific Publishing Co., California, USA (2007). https://doi.org/10.1142/p444

[14] Brown, E.L., Petersen, K.D., Lesher, C.E.: Markov Chain Monte Carlo inversion of mantle temperature and source composition, with application to Reykjanes Peninsula, Iceland. Earth and Planetary Science Letters **532**, 116007 (2020) https://doi.org/10.1016/j.epsl.2019.116007

[15] Oliveira, B., Afonso, J.C., Klöcking, M.: Melting conditions and mantle source composition from probabilistic joint inversion of major and rare earth element concentrations. Geochimica et Cosmochimica Acta **315**, 251–275 (2021) https://doi.org/10.1016/j.gca.2021.09.008

[16] Misra, K.C.: Introduction to Geochemistry: Principles and Applications. John Wiley & Sons, Oxford, UK (2012)

[17] Maaløe, S.: Estimation of the degree of partial melting using concentration ratios. Geochimica et Cosmochimica Acta **58**(11), 2519–2525 (1994) https://doi.org/10.1016/0016-7037(94)90028-0

[18] Zou, H., Zindler, A.: Constraints on the degree of dynamic partial melting and source composition using concentration ratios in magmas. Geochimica et Cosmochimica Acta **60**(4), 711–717 (1996) https://doi.org/10.1016/0016-7037(95)00434-3

[19] Treuil, M., Joron, J.-L.: Utilisation des elements hygromagmatophiles pour la simplifications de la modelisation quantitative des precessus magmatiques. Soc. Ital. Mineral. Petrol. **31**(0001), 125–174 (1975)

[20] Minster, J., Allègre, C.: Systematic use of the trace elements in igneous processes. Contributions to Mineralogy and Petrology **68**(1), 37–52 (1978) https://doi.org/10.1007/BF00375445

[21] Albarède, F.: Inversion of batch melting equations and the trace element pattern of the mantle. Journal of Geophysical Research: Solid Earth **88**(B12), 10573–10583 (1983) https://doi.org/10.1029/JB088iB12p10573 https://agupubs.onlinelibrary.wiley.com/doi/pdf/10.1029/JB088iB12p10573

[22] Hofmann, A.W., Feigenson, M.D.: Case studies on the origin of basalt. Contributions to Mineralogy and Petrology **84**(4), 382–389 (1983) https://doi.org/10.1007/BF01160289

[23] Ormerod, D., Rogers, N., Hawkesworth, C.: Melting in the lithospheric mantle: Inverse modelling of alkali-olivine basalts from the Big Pine Volcanic Field, California. Contributions to Mineralogy and Petrology **108**(3), 305–317 (1991) https://doi.org/10.1007/BF00285939

[24] Feigenson, M.D., Carr, M.J.: The source of Central American lavas: inferences from geochemical inverse modeling. Contributions to Mineralogy and Petrology **113**, 226–235 (1993) https://doi.org/10.1007/BF00283230

[25] Cebriá, J.-M., López-Ruiz, J.: A refined method for trace element modelling of nonmodal batch partial melting processes: The Cenozoic continental volcanism of Calatrava, central Spain. Geochimica et Cosmochimica Acta **60**(8), 1355–1366 (1996) https://doi.org/10.1016/0016-7037(96)00017-8

[26] Caroff, M., Maury, R., Guille, G., Cotten, J.: Partial melting below Tubuai (Austral Islands, French Polynesia). Contributions to Mineralogy and Petrology **127**, 369–382 (1997) https://doi.org/10.1007/s004100050286

[27] Velasco-Tapia, F., Verma, S.P.: First partial melting inversion model for a rift-related origin of the Sierra de Chichinautzin Volcanic Field, Central Mexican Volcanic Belt. International Geology Review **43**(9), 788–817 (2001) https://doi.org/10.1080/00206810109465048 https://doi.org/10.1080/00206810109465048

[28] Velasco-Tapia, F., Verma, S.P.: Magmatic processes at the volcanic front of Central Mexican Volcanic Belt: Sierra de Chichinautzin Volcanic Field (Mexico). Turkish Journal of Earth Sciences, 32–60 (2013) https://doi.org/10.3906/tar-1202-35

[29] Feigenson, M.D., Bolge, L.L., Carr, M.J., Herzberg, C.T.: REE inverse modeling of HSDP2 basalts: Evidence for multiple sources in the Hawaiian plume. Geochemistry, Geophysics, Geosystems **4**(2) (2003) https://doi.org/10.1029/2001GC000271 https://agupubs.onlinelibrary.wiley.com/doi/pdf/10.1029/2001GC000271

[30] Verma, S.: Solely extension-related origin of the eastern to west-central Mexican Volcanic Belt (Mexico) from partial melting inversion model. Current Science **86**, 713–719 (2004)

[31] Verma, S.P.: Extension-related origin of magmas from a garnet-bearing source in the Los Tuxtlas volcanic field, Mexico. International Journal of Earth Sciences **95**(5), 871–901 (2006) https://doi.org/10.1007/s00531-006-0072-z

[32] Williams, H.M., Turner, S.P., Pearce, J.A., Kelley, S.P., Harris, N.B.W.: Nature of the source regions for post-collisional, potassic magmatism in southern and northern tibet from geochemical variations and inverse trace element modelling. Journal of Petrology **45**(3), 555–607 (2004) https://doi.org/10.1093/petrology/egg094 https://academic.oup.com/petrology/article-pdf/45/3/555/4200660/egg094.pdf

[33] Clague, D.A., Frey, F.A.: Petrology and Trace Element Geochemistry of the Honolulu Volcanics, Oahu: Implications for the Oceanic Mantle below Hawaii. Journal of Petrology **23**(3), 447–504 (1982) https://doi.org/10.1093/petrology/23.3.447 https://academic.oup.com/petrology/article-pdf/23/3/447/4306122/23-3-447.pdf

[34] Giannetti, B., Ellam, R.: The primitive lavas of Roccamonfina volcano, Roman region, Italy: new constraints on melting processes and source mineralogy. Contributions to Mineralogy and Petrology **116**(1-2), 21–31 (1994) https://doi.org/10.1007/BF00310687

[35] Singh, P., Choudhary, S.K.: Introduction: Optimization and metaheuristics algorithms. In: Malik, H., Iqbal, A., Joshi, P., Agrawal, S., Bakhsh, F.I. (eds.) Metaheuristic and Evolutionary Computation: Algorithms and Applications, pp. 3–33. Springer, Singapore (2021). https://doi.org/10.1007/978-981-15-7571-6_1 . https://doi.org/10.1007/978-981-15-7571-6_1

[36] Yang, X.-S.: Engineering Optimization: An Introduction with Metaheuristic Applications. John Wiley & Sons, New Jersey, USA (2010)

[37] Silva Pereira, J.a.E., Strieder, A.J., Amador, J.P., Silva, J.L.S., Volcato Descovi Filho, L.L.: A heuristic algorithm for pattern identification in large multivariate analysis of geophysical data sets. Comput. Geosci. **36**(1), 83–90 (2010) https://doi.org/10.1016/j.cageo.2009.03.009

[38] Haddad, O.B., Tabari, M.M.R., Fallah-Mehdipour, E., Mariño, M.: Groundwater model calibration by meta-heuristic algorithms. Water resources management **27**(7), 2515–2529 (2013) https://doi.org/10.1007/s11269-013-0300-9

[39] Yoo, D.G., Kim, J.H.: Meta-heuristic algorithms as tools for hydrological science. Geoscience Letters **1**(4), 2196–4092 (2014) https://doi.org/10.1186/2196-4092-1-4

[40] Neupane, R., Datta, B.: Optimal characterization of unknown multispecies reactive contamination sources in an aquifer. Journal of Hydrologic Engineering **26**(11), 04021035 (2021) https://doi.org/10.1061/(ASCE)HE.1943-5584.0002134

[41] Shin, J.-Y., Heo, J.-H., Jeong, C., Lee, T.: Meta-heuristic maximum likelihood parameter estimation of the mixture normal distribution for hydro-meteorological variables. Stoch Environ Res Risk Assess 28 **28**(6425), 347–358 (2014) https://doi.org/10.1007/s00477-013-0753-7

[42] Aguirre-López, M.A., Soto-Villalobos, R., Casas-Ramírez, M.-S., Almaguer, F.-J.: A comparative study on using metaheuristics for the seismic-ray-tracing problem. Earth Science Informatics **14**(1), 469–483 (2021) https://doi.org/10.1007/s12145-020-00549-3

[43] D'Amico, S., Cacciola, M., Parrillo, F., Carlo Morabito, F., Versaci, M., Barrile, V.: Heuristic advances in identifying aftershocks in seismic sequences. Computers & Geosciences **35**(2), 245–254 (2009) https://doi.org/10.1016/j.cageo.2008.03.010

[44] Poormirzaee, R., Moghadam, R.H., Zarean, A.: Inversion seismic refraction data using particle swarm optimization: a case study of Tabriz, Iran. Arabian Journal of Geosciences **8**(8), 5981–5989 (2015) https://doi.org/10.1007/s12517-014-1662-x

[45] Poormirzaee, R., Sarmady, S., Sharghi, Y.: A new inversion method using a modified bat algorithm for analysis of seismic refraction data in dam site investigation. Journal of Environmental and Engineering Geophysics **24**(2), 201–214 (2019) https://doi.org/10.2113/JEEG24.2.201

[46] Chen, Y., An, A.: Application of ant colony algorithm to geochemical anomaly detection. Journal of Geochemical Exploration **164**, 75–85 (2016) https://doi.org/10.1016/j.gexplo.2015.11.011

[47] Emmerich, M., Shir, O.M., Wang, H.: Evolution strategies. In: Martí, R., Pardalos, P.M., Resende, M.G.C. (eds.) Handbook of Heuristics, pp. 1–31. Springer, Cham, Switzerland (2018). https://doi.org/10.1007/978-3-319-07153-4_13-1 . https://doi.org/10.1007/978-3-319-07153-4_13-1

[48] Conover, W.J.: Practical Nonparametric Statistics. John Wiley & Sons, New York, USA (1999)

[49] Arndt, N.T.: Ultrabasic magmas and high-degree melting of the mantle. Contributions to Mineralogy and Petrology **64**, 1432–0967 (1977) https://doi.org/10.1007/BF00371512

[50] Govindaraju, K.: 1994 compilation of working values and sample description for 383 geostandards. Geostandards Newsletter **18**(S1), 1–158 (1994) https://doi.org/10.1046/j.1365-2494.1998.53202081.x-i1 https://onlinelibrary.wiley.com/doi/pdf/10.1046/j.1365-2494.1998.53202081.x-i1

[51] Pearce, J.A., Barker, P., Edwards, S., Parkinson, I.J., Leat, P.: Geochemistry and tectonic significance of peridotites from the South Sandwich arc–basin system, South Atlantic. Contributions to Mineralogy and Petrology **139**(1), 36–53 (2000) https://doi.org/10.1007/s004100050572

[52] McKenzie, D., O'nions, R.K.: Partial melt distributions from inversion of Rare Earth Element concentrations. Journal of Petrology **32**(5), 1021–1091 (1991) https://doi.org/10.1093/petrology/32.5.1021 https://academic.oup.com/petrology/article-pdf/32/5/1021/4327457/32-5-1021.pdf

[53] Torres-Alvarado, I.S., Verma, S.P., Palacios-Berruete, H., Guevara, M., González-Castillo, O.Y.: DC_BASE: a database system to manage nernst distribution coefficients and its application to partial melting modeling. Computers & Geosciences **29**(9), 1191–1198 (2003) https://doi.org/10.1016/S0098-3004(03)00132-8

[54] Nakamura, N.: Determination of REE, Ba, Fe, Mg, Na and K in carbonaceous and ordinary chondrites. Geochimica et Cosmochimica Acta **38**(5), 757–775 (1974) https://doi.org/10.1016/0016-7037(74)90149-5

[55] Haskin, L.A., Haskin, M.A., Fredy, F.A., Wildeman, T.R.: Relative and absolute terrestrial abundances of the rare earths. In: Ahrens, L.H. (ed.) Origin and Distribution of the Elements. International Series of Monographs in Earth Sciences, pp. 889–912. Pergamon, Oxford, UK (1968). https://doi.org/10.1016/B978-0-08-012835-1.50074-X